

Computer Vision Segmentation of Brain Structures from MRI Based on Deformable Contour Models

Ladan Amini^{a,b}, Hamid Soltanian-Zadeh^{a,b,c}, Caro Lucas^{a,b}

^aElec. and Comp. Eng. Dept., Faculty of Eng., Univ. of Tehran, Tehran, Iran

^bInstitute for Studies in Theoretical Physics and Mathematics, Tehran, Iran

^cRadiology Dept., Henry Ford Health System, Detroit, Michigan, USA

Abstract: Based on a discrete dynamic contour model, a method for segmentation of brain structures like thalamus from magnetic resonance images (MRI) is developed. A new method for solving common problems in extracting the discontinuous boundary of a structure from a low contrast image is presented. External and internal forces deform the dynamic contour model. Internal forces are obtained from local geometry of the contour, which consist of vertices and edges, connecting adjacent vertices. The image data and desired image features such as image energy are utilized to obtain external forces. The problem of low contrast image data and unclear edges in the image energy is overcome by a new algorithm that uses several methods like thresholding, unsupervised clustering methods such as fuzzy C-means (FCM), edge-finding filters like Prewitt, and morphological operations. We also present a method for generating an initial contour for the model from the image data automatically. Evaluation and validation of the methods are conducted by comparing automatic and radiologist segmentation results, which confirms good performance of the new method.

Keywords: Dynamic contours; Clustering; Segmentation; Image processing; Thalamus; MRI

1. Introduction

One of the most important neuro-anatomic structures is thalamus. The thalami are the largest, most internal structures of the diencephalon, consisting of two oblique ovoid nuclear masses of gray matter situated at the rostral end of the mid brain on each side of the third ventricle. Each thalamus is about 3-4 cm long [1]. Thalamus is the gathering center of sensory and conceptual signals and tunes them. Motor nuclei of the thalamus receive signals from the striatum and cerebellum and project into the motor and premotor areas of the cerebral cortex. The thalamus has a key function in the sensory systems [2]. Thalamus specifications like its volume or its intensity on MR images are expected to change by many neurological diseases.

Thalamus has relatively low contrast and discontinues edges. These difficulties complicate the accurate automatic segmentation of the thalamus. Manual segmentation requires extensive human interaction and considerable training, and both intra-rater reproducibility and inter-rater reliability may be difficult to achieve. Segmentation of the

thalamus with conventional methods, such as edge tracking, thresholding or region growing individually is not reliable because of low contrast and discontinuous edges of the thalamus. Deformable models seem more appropriate than conventional segmentation and standard edge detection methods [3], due to their relative power in treating each structure as a unit object, producing a closed contour, and their flexibility. The result of deformable models segmentation depends on the operator that generates the initial contour. To overcome this difficulty we have generated the initial contour by a new algorithm. The new algorithm uses fuzzy c-means (FCM) clustering [4,5], thresholding, and morphological operations.

2. Background

Active contour models, first introduced by Kass, Witkin and Terzopoulos [6,7] and have been investigated and applied in various ways. Terzopoulos' snake model minimizes the energy of spline segments of a contour. Active contour models are often referred to as the classic snake or deformable contour model. They are energy-minimizing splines guided by internal shape forces, external constraint forces, and external image forces like edges that pull them towards image features during an optimization process. They dynamically segment an image by locking onto nearby edges and localizing them accurately.

Over the past decade, a considerable amount of research has been done concerning different aspects of these deformable models. Different authors have used different methods for solving differential equations related to the contour evolution [8]. The models that use differential methods for minimizing the contour energy (e.g. [6,7]) are computationally inefficient and can lead to numerical instability, due to the discrete nature of the image. In contrast, several authors have used different dynamic programming methods. Geiger *et al.* [9] and Amini *et al.* [10] have used dynamic programming for tracking and matching the deformable contours and minimizing its energy, Grzeszczuk and Levin [11] used simulated annealing [12] for evolution of the contour, to make the model stable. They have incorporated statistical region-based image features to improve the reliability of the algorithm and used it in multi-region segmentation. Some of the authors used analytical or parametric models to represent a contour (see Refs [13]). Although this makes the model more compact and is useful for applications such as motion analysis [14], structures with irregular shapes and sharp corners cannot be easily represented by these models and may need a large number of terms and a considerable increase in calculations. In contrast, discrete models seem to be more flexible in fitting into edges with high curvature [15]. Leitner and Cinquin [16] have redefined internal forces and used the results for 3D segmentation.

Researchers have used deformable contours for segmentation and identification of structures from MR brain images [17], like hippocampus [18-20]. Lobregt and Viergever [21] have introduced a new discrete dynamic contour model. Their model is not well suited for segmentation of low-contrast images. They have introduced a damping force for stabilizing the contour, but it is hard to find proper weighting for this force from image to image or within different areas of an image. Also, this force cannot always make the contour stable without decreasing its accuracy. Ghanei *et al.* [18] followed the geometry introduced in [21], but they have redefined external forces by using an edge-tracking method. They have addressed the problems associated with optimizing the internal force weight and contour stability. The external force, which pulls the dynamic contour towards the object edge, is equal to the inverse of the gradient of the image energy.

They have applied standard edge finding methods on the image data to get the image energy, but this image energy is not always appropriate for deriving external forces, because

of low-contrast image data and therefore unclear and discontinuous edges in the image energy. Due to the low variation of gradient in the edge position of the above image energies, the external force will not move the contour. Also, their segmentation is semi automatic and the result depends on the operator due to generating initial contour. Our work follows the geometric model introduced in [21] and [18], but we have improved the external image energy to segment thalamus by a new algorithm. The new algorithm has overcome the difficulties that obtaining image energy had by using FCM clustering, thresholding and morphological operators. We have also presented a new algorithm to generate the initial contour to reduce the dependency of the segmentation results on the operator.

3. Discrete Contour Model

In this section, first, the basic structure of the model and force fields [21] are presented. Then, some improvements in the model and changes introduced into the deformation process and the image energy [18] are briefly described.

3.1. Model Structure

The geometric structure of model (see Figure 1) and force fields are explained here. The dynamic model is a contour consisting of vertices, which are connected by straight segments. The position of a vertex is represented by a vector P_i . The unit vector in the direction of the edge (D_i) between vertices is shown by d_i . The unit tangential vector at vertex i is t_i , where t_i is:

$$t_i = \frac{d_{i-1} + d_i}{\|d_{i-1} + d_i\|} \quad (1)$$

By rotating the tangential vector 90° clockwise, the radial vector, r_i , is attained. Each vertex moves along its radial vector during the deformation. The movement of the snake is started from an initial contour. Vertices deform according to the sum of the internal, external, and a damping force. The internal force, $f_{in,i}$, causes the dynamic contour model to be smoother and less flexible and is calculated from the curvature of the contour. Curvature is determined at a vertex as the vector difference between the unit tangential vectors of two joining edge segments:

$$c_i = d_i - d_{i-1} \quad (2)$$

The internal force is driven from the curvature value at vertices convolved with an appropriate filter, $k_i = \{\dots, 0, 0, -1/2, 1, -1/2, 0, 0, \dots\}$, to prevent changes in parts of the contour with average curvature of zero:

$$f_{in,i} = (c_i \otimes k_i) r_i \quad (3)$$

The external force is responsible for pulling the model near the desired local energy minimum or the edges. The external force, $f_{ex,i}$ is driven from the image features. For calculating the external force, we have

$$f_{ex,i} = (r_i \cdot f_{im}(x_i, y_i)) r_i \quad (4)$$

where (x_i, y_i) is the position of vertex i and $f_{im}(\cdot)$ is gradient vector of the image feature.

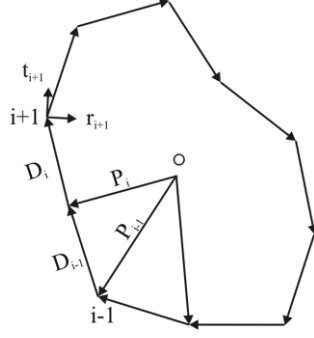


Figure 1. The geometric model consists of a set of vertices such as i that is represented by vector P_i and is connected by edge D_i . A radial vector r_i and a tangential vector t_i are defined for each

The damping force, $f_{damp, i}$, is set proportional to the square of the vertex speed. Applying some weights to internal and external forces determine the smoothness of the result and whether the contour chases the image feature in exact way or in global way or between two. The dynamic contour moves to perform a coarse to fine tracking of image features, iteratively. In each iteration, a resampling over contour is done to avoid having too large or too short segments.

3.2. Improved External Forces

A method is presented in [18] to avoid the contour trapping at undesired edges or undesired local minimum energies. In this method, for each vertex, i , an edge is searched within a specified distance along radial vector r_i . Each point on r_i can be represented by a parametric vector such as $s_{\alpha, i} = p_i - \alpha r_i$. α is changed between $-\alpha_{max}$ to α_{max} with steps $\Delta\alpha$ moving $s_{\alpha, i}$ along r_i to search from a specified distance inside to outside of the object. In this search, the contour may be trapped in the opposite border instead of the correct border. To solve this problem we change α between 0 and α_{max} to move $s_{\alpha, i}$ along r_i from the vertices of the contour to the object edge. After finding an edge based on a local minimum of the external energy, the external force is calculated which is pointing toward the edge location. If no local minimum of the external energy is found the external force is set zero. The above model let the user attach springs between the vertices of the contour and the object edge. Therefore, the external force pulls the contour vertices toward the edge on the image energy. To complete equation (4) in order to calculate the external force, we have

$$f_{ex, i} = \beta ((s_{min, j} - p_i) \cdot r_i) r_i = -\beta \alpha_{min} r_i \quad (5)$$

where β is a positive constant that normalizes the length of the external force, $s_{min, j}$ is the point where the local minimum or the edge is found, and $s_{min, j}$ equals $p_i - \alpha_{min} r_i$.

4. Proposed Methods

4.1. Improved External Image Energy

Here, we describe the deformation process to specify the importance of the image energy. The deformation process starts from an initial contour. For each vertex of the contour, along

radial vector is searched to find an edge. A location on radial vector is interpreted as edge, if the external energy has a minimum at that location. This search is continued until a local minimum of the energy is found. The external force pulls the vertex towards the edge location. If no edge is found the external force is set zero. The deformation process is ended automatically when all the vertices is stopped or when the number of iterations exceeds a limit. Each vertex is stopped when the length of its external force become small. The convergence has defined in [21] when the velocity, acceleration, and sum of forces of all vertices become zero that is time consuming.

Using the gradient of the image intensity or other standard edge finding methods may be appropriate for some applications. However, since thalamus has a relatively low contrast, low signal to noise ratio (SNR) and discontinues edge, well-improved image energy is required for extracting the desired image features to move the contour toward the edge object. Due to the mentioned difficulties that thalamus in MR images possesses, the image energy that is derived from the standard edge finding methods like Prewitt method [22] is not applicable for thalamus. We have developed a new algorithm to solve this problem. The improved image energy finder (IIEF) algorithm is as follows:

1. The Prewitt method is used to obtain the basic image energy. Prewitt method finds edges using the Prewitt approximation to the derivative. It returns edges at those points where the gradient of image intensity is a maximum. The basic image energy is shown in Figure 2(a).

2. A binary image is created from the original intensity image based on the user-defined luminance threshold. We have used a value of 0.3 as threshold in our experiments. The binary map is overlaid on the prewitt-filtered image to make the strong edges sharp. The results are depicted in Figure 2(b).

3. Since thalamus is almost entirely a gray matter (GM) structure, we calculate the edge map of GM and expect the contour to finally converge to the desired GM boundaries. For extracting the GM boundaries FCM (ref, to Appendix) is applied on the original image with fuzzification degree equal to 1.7 and the number of clusters equal to 6 (see Figure 2(c)). Fuse clusters that include GM to obtain a better and more detailed representation of the GM edges around the thalamus. Figure 2(d) displays the result of fusing.

4. The GM edge map is eroded to remove the gray matter regions around the thalamus from its structure. The structuring element have been used for erosion is a 3×3 matrix containing only 1's. Connected components are labeled in binary image and dilate the results with the same structuring element to obtain a detailed representation of the shape of thalamus in an isolated cluster. (see Figure 2(e))

5. Each pixel is set to zero if its 4-connected neighbors are all 1's, thus leaving only boundary pixels of the thalamus. The acquired boundary map is overlaid on the result of step 2 (see Figure 2(f)).

6. For the algorithm to be effective in finding the thalamus in all the layers of the brain MR images, midline should be used. It is important to note that the two thalami often connected across the midline by the massa intermedia [23]. In images which two thalami are linked together, midline should be obtained to separate the thalami (Figure 2(g)).

7. Due to dealing with discrete image energy the final contour will oscillate if there are two states with minimum energy for the contour. To avoid this problem, the image energy is interpolated by a bilinear function to generate a continuous map. The result is shown in Figure 2(h).

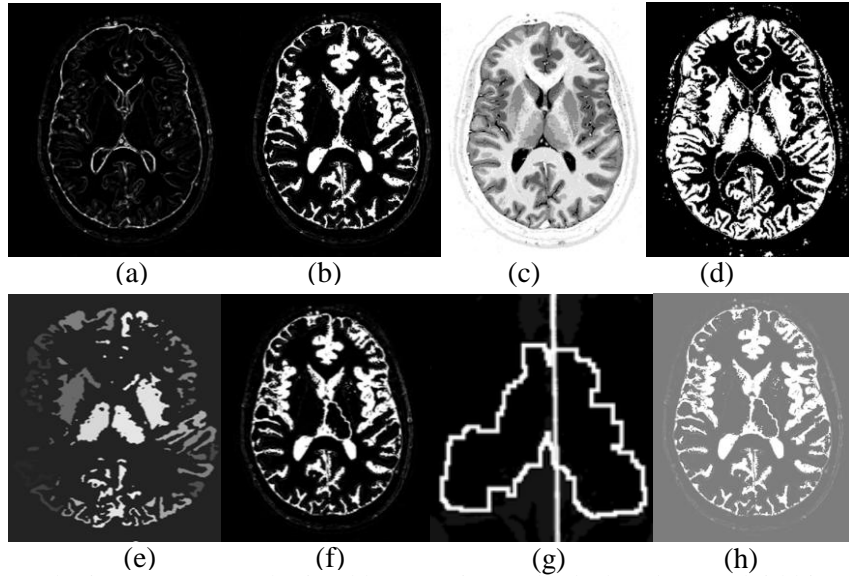


Figure 2. (a) The image energy obtained by Prewitt method; (b) The overlaid binary map on the basic image energy (part a); (c) FCM clustering result; (d) Result of fusing clusters that include thalamus; (e) Result of Labeling connected components in the gray matter edge map; (f) Overlaid the coarse boundary of thalamus on the semi-improved image energy obtained in step 2 of section 4.1; (g) Mid line separated thalami; (h) Interpolated improved image energy.

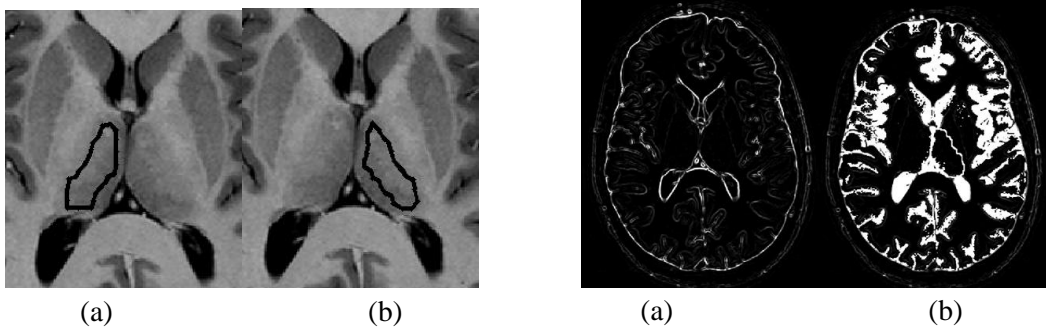


Figure 3. The initial contour for the thalamus of (a) left and (b) right side of the image.

Figure 4. The image energy obtained by (a) prewitt method and (b) the new method (IIEF, Section 4.1)

4.2. Generation of Initial Contour

The deformation process starts from an initial contour. To eliminate dependency of segmentation results from operator, we have developed a method to generate the initial contour. For this purpose, first we erode the boundary map acquired at step 5 of the IIEF algorithm; the structuring element of the erosion used in our experiments is a 5×5 matrix containing only 1's. Then, we decrease the number of the points on the boundary map by a down sampling. The down sampling rate specifies the number of the points the user desires to have on the initial contour (see Figure 3).

5. Experimental Results

We have developed a method based on discrete contour model to segment thalamus and similar objects of interest from brain MRI. For this purpose, we have proposed a new method to extract the desired image features and developed an algorithm to automate definition of the

initial contour to overcome the problem of dependency of results on the operator. Automating segmentation of specific brain structures from MRI increases the advantages of the model over semi-automatic and manual segmentation in regard to speed, easiness, reproducibility and independency of results on the operator. The initial contours are successfully extracted from the original image adaptively, as are shown as black contours in Figure 3.

Using standard edge-finding methods such as step expansion filter (SEF), gradient of the image gray levels and Prewitt methods are not appropriate for our application. Since the thalamus has a relatively low contrast, low signal-to-noise ratio (SNR) and discontinues edge, the image energy derived from the standard edge finding methods alone, e.g., Prewitt method, is not applicable. Improved image energy is required for extracting the desired image features to move the contour towards the object edge. Figure 4 compares the result of Prewitt filtered image and the improved image energy. Note that extracting the desired features is almost impossible using the Prewitt filter itself (Figure 4(a)). However, in the improved image energy, the desired image features, needed for calculating the external forces to move the contour towards the real edges of thalamus, are extracted from the original image. The problems of extracting desired features due to low contrast and low SNR that causes unclear and discontinuous edges in the Prewitt image energies have been overcome by using fuzzy clustering, thresholding and morphological operations. The parameters of the dynamic contour can be fixed for a wide range of applications, once the designer finds optimal values for them.

Figure 5 shows the result of thalamus segmentation using the dynamic contour model and the improved image energy. It also shows the manual segmentation results generated by an expert radiologist. We use the Tanimoto similarity measure [4] to quantitatively evaluate the experimental results. This measure quantifies the similarity between two discrete-valued vectors x and y . It is defined as:

$$S_T(x, y) = \frac{a_{11}}{a_{11} + a_{01} + a_{10}} \quad (6)$$

where the element a_{ij} is the number of places where the first vector has the i symbol and the corresponding element of the second vector has the j symbol, $i, j = 0, 1$. The values of the calculated Tanimoto similarity measure between the segmented regions are listed in Table 1, which illustrates excellent agreement between the automatic and manual segmentation results.

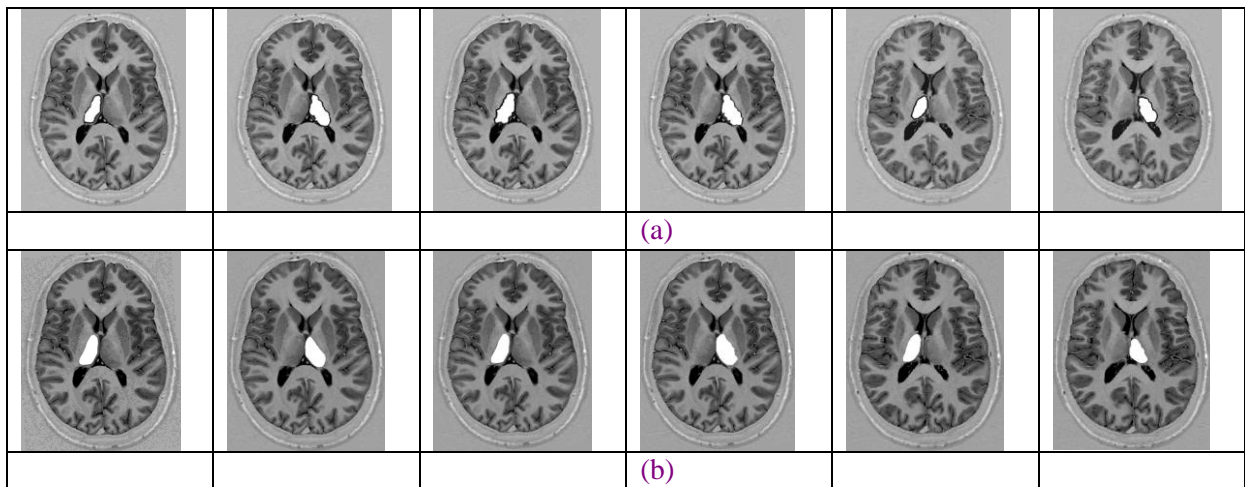


Figure 5. (a) Automatic segmentation and (b) Radiologist's segmentation results overlaid on three brain slices.

Table 1. Number of common and uncommon (different) pixels and similarity of the segmentations generated by the expert radiologist and the proposed automatic method for six brain slices (SL10-SL13) that include thalamus, acquired from two subjects (Case1, Case2).

Slices	a_{11}	a_{10}	a_{01}	Similarity between automatic and expert segmentation
Left thalamus				
Case1-SL10	1550	410	139	0.74
Case1-SL11	2079	63	146	0.91
Case1-SL12	1118	31	98	0.90
Case2-SL11	1229	23	225	0.83
Case2-SL12	1721	126	83	0.90
Case2-SL13	1069	125	324	0.70
Right thalamus				
Case1-SL10	1705	343	98	0.80
Case1-SL11	1843	48	96	0.93
Case1-SL12	1047	13	202	0.83
Case2-SL11	1620	244	57	0.84
Case2-SL12	1624	152	157	0.84
Case2-SL13	1417	108	74	0.89

6. Summary

We have investigated the problem of segmenting thalamus from brain MRI. Thalami have a key function in the sensory system due to processing information before forwarding it to the select area of the cerebral cortex. Thalami play an important role in the maintenance and regulation of the state of consciousness, alertness, and also possibly attention [23].

Segmentation of thalamus and its specifications like its volume is expected to be influential in noninvasive diagnosis of some important neurological diseases. We have developed an improved dynamic contour model for this purpose. We have solved the problem of low contrast, low SNR and discontinuous edges of thalamus in MRI that causes uncertain and discontinuous edges in the image energies. This has been done by a new algorithm that generates appropriate image energy for our application and similar patterns. It helps the contour to be absorbed to the real edges of the object of interest. Also, the difficulty of the dependency of the result of dynamic contour models on the operator has been overcome by introducing a method for generating the initial contour automatically. Finally, the described methods have been tested on real clinical brain MRI and results showed a very good performance.

Acknowledgment

We would like to thank Dr. Gity (Staff Radiologist, Imam Khomeini Hospital, University of Tehran Medical School, Tehran, Iran) for manual segmentation of thalamus and Dr.

Akhlaghpour (Staff Radiologist, Novin Imaging Center, Tehran, Iran) and Mrs. Nasim Maleki for their helps in preparing images.

Appendix

The FCM is a data clustering technique where each data point (intensity of each pixel) belongs to a cluster to some degree specified by a membership value. It starts with an initial guess for the cluster centers, which are intended to mark the mean location of each cluster, and iteratively moves the centers to the right location within the data set. The optimization process is based on minimizing an objective function that represents the distance from any given pixel intensity to a cluster center weighted by the related membership value. The number of clusters and the fuzzification degree are two of the FCM algorithm inputs.

References

- [1] J. C. Tamraz, Y. G. Comair, "Atlas of regional anatomy of the brain using MRI with functional correlations," Springer-Verlag Berlin Heidelberg, 2000
- [2] V. Barra, J. Y. Boire, "Automatic segmentation of subcortical brain structures in MR images using information fusion," *IEEE Trans. Med. Img.*, 2001;20:549-558.
- [3] O. Faugeras, "Three dimensional computer vision: a geometric view point," Cambridge MA: MIT Press., 1993.
- [4] S. Teodiridis, K. Kourtoumbas, "Pattern recognition," Academic Press, 1998.
- [5] A. K. Jain, R. P. W. Duin, J. Mao, "Statistical pattern recognition: a review," *IEEE Trans. Pat. Ana. & Mach. Intell.*, 2000;22(1).
- [6] D. Terzopoulos, J. Platt, A. Barr, K. Fleischer, "Elastically deformable models," *Comput. Graph.*, 1987;21(4):205-214.
- [7] M. Kass, A. Witkin, D. Terzopoulos, Snakes: "active contour models," *Int. Comput. Vision*, 1988;321-331.
- [8] C. Davatzikos, R. N. Bryan, "Using a deformable surface to obtain a shape representation of the cortex," *IEEE Trans. Med. Imag.*, 1996; 15(6): 785-795.
- [9] D. Geiger, A. Gupta, L. A. Costa, J. Vlontzos, "Dynamic programming for detecting tracking and matching deformable contours," *IEEE Trans. Patt. Anal. Mach. Intell.*, 1995;17:294-302.
- [10] A. A. Amini, T.E. Weymouth, D. J. Anderson, "A parallel algorithm for determining two dimensional object positions using incomplete information about their boundaries," *Patt. Recog.*, 1989;22:21-28.
- [11] P. Grzeszczuk, D. N. Levin, "Brownian strings: segmenting images with stochastically deformable contours," *SPIE*, 1994;2359:72-89.
- [12] P. M. Pardalos, M. G. C. Resende, "Handbook of applied optimization," Oxford University Press, 2002.
- [13] G. Szekely, A. Kelemen, C. Brechbuhler and G. Gerig, "segmentation of 2-D and 3-D objects from MRI volume data using models," *Med. Imag. Anal.*, 1996;1(1):19-34.
- [14] D.L. Guidry, A. A. Farag, "Using Active Contours and Fourier descriptors for motion tracking with applications in MRI," *IEEE*, 1999.
- [15] S. Matsumoto, R. Asato, T. Okada, J. Konishi, "Intracranial contour extraction with active contour models," *JMIR*, 1997;7:353-360.
- [16] F. Leinter, P. Cinquin, "From splines and snakes to snake splines," *Workshop: Geometric Reasoning for Perception and Action* 264-281; 1993.

- [17] C. Davatzikos, J. L. Prince, "Brain image registration based on curve mapping," Proc. IEEE Workshop Biomed. Imag. Los Alamitos CA USA., 1994;245-254.
- [18] A. Ghanei, H. Soltanian Zadeh, J. P. Windham, "Segmentation of the hippocampus from brain MRI using deformable contours," Computerized Med. Imag. and Graphics, 1998;22:203-216.
- [19] A. Ghanei, H. Soltanian Zadeh, J. P. Windham, "A deformable model for hippocampus segmentation: improvements and extension to 3D," Computer in Biology and Medicine, 1998;28:239-258.
- [20] D. Shen, S. Moffat, S. M. Resnick, C. Davatzikos, "Measuring size and shape of the hippocampus in MR images using a deformable shape model," Neuroimag, in Press.
- [21] S. Lobregt, M. A. Viergever, "A discrete dynamic contour model," IEEE Trans. Med. Imag., 1995;14(1):12-24.
- [22] J. R. Parker, "Algorithms for image processing and computer vision," New York, John Wiley & Sons Inc., 1997;23-29.
- [23] W. J. Hendelman, "Atlas Functional Neuroanatomy," CRC Press LLC, 2000.